LAWRENCE
LIVERMORE
NATIONAL
LABORATORY

LLNL-JRNL-413708

Measurements of the critical power for self-injection of electrons in a laser wakefield accelerator

D. H. Froula, C. E. Clayton, T. Doppner, R. A. Fonseca, K. A. Marsh, C. J. Barty, L. Divol, S. H. Glenzer, C. Joshi, W. Lu, S. F. Martins, P. Michel, W. Mori, J. P. Palastro, B. B. Pollock, A. Pak, J. E. Ralph, J. S. Ross, C. Siders, L. O. Silva, T. Wang

June 8, 2009

Physcial Review Letters

Disclaimer

Measurements of the critical power for self-injection of electrons in a laser wakefield accelerator

D. H. Froula[1],* C. E. Clayton[2], T. Döppner[1], R. A. Fonseca[4], K. A. Marsh[2], C. J. Barty[1], L. Divol[1], S. H. Glenzer[1], C. Joshi[2], W. Lu[2], S. F. Martins[4], P. Michel[1], W. Mori[2], J. P. Palastro[1], B. B. Pollock[1,3], A. Pak[2], J. E. Ralph[1,2], J. S. Ross[1,3], C. Siders[1], L. O. Silva[4], and T. Wang[2]

[1] *L-399, Lawrence Livermore National Laboratory, P.O. Box 808, Livermore, CA 94551, USA*

[2] *Department of Electrical Engineering, University of California, Los Angeles, CA 90095*

[3] *Department of Mechanical and Aerospace Engineering, University of California, San Diego, 9500 Gilman Dr., La Jolla, CA 92093 and*

[4] *GoLP/Instituto de Plasmas e Fusão Nuclear, Instituto Superior Técnico, Lisbon, Portugal*

(Dated: June 2, 2009)

A laser wakefield acceleration study has been performed in the matched, self-guided, blow-out regime where a 10 J, 60 fs laser produced 720 ± 50 MeV quasi-monoenergetic electrons with a divergence of $\Delta\theta = 2.85 \pm 0.15$ mRad. While maintaining a nearly constant plasma density (3×10^{18} cm^{-3}), a linear electron energy gain was measured from 100 MeV to 700 MeV when the plasma length was scaled from 3 mm to 8 mm. Absolute charge measurements indicate that self-injection occurs when $P/P_{cr} > 4$ and saturates around 100 pC for $P/P_{cr} > 12$. The results are compared with both analytical scalings and full 3D particle-in-cell simulations.

PACS numbers: 52.38.Kd, 41.75.Jv, 52.35.Mw
Keywords:

Thirty years ago Tajima and Dawson predicted that a plasma wave driven by an intense laser pulse can produce 10-100 GeV/m electric fields which could accelerate electrons [1]. More than a decade later, laser-accelerator experiments used beam waves and the Raman forward instability to drive large amplitude plasma waves that generated electrons beams with a thermal tail reaching high energies [2–6]. It was not until the laser technology advanced to having a sufficiently short pulse duration, at powers above 10 TW, that $\sim$ 100 MeV quasi-monoenergetic electron beams were realized [7–9].

The ponderomotive force of an ultra-short ($t \sim 2\pi/\omega_p$) relativistically intense laser pulse propagating through an under-dense plasma can completely blow out the electrons forming a spherical ion column behind the pulse of the laser [10, 11]. Electrons along the sheath of the sphere are pulled towards the laser axis and cross at the rear. Electron residing within the region of high accelerating and focusing fields can be self injected into the accelerating structure when they gain enough momentum to catch up with the wake of laser. These self-injected electrons are then accelerated until they either outrun the slower moving laser pulse over a "dephasing length" or the laser intensity is reduced below the blow-out threshold. To maintain intensity of the laser beam over many Rayleigh lengths the diffraction of the laser field can be balanced with refraction in a self-generated electron density channel provided the laser power is greater than the critical power for self-focusing ($P_{cr} = 17\omega_0^2/\omega_p^2$ GW) [12–16].

In order to increase the electron energy beyond the initial 100 MeV results [13], the dephasing length must be increased by reducing the density ($L_{dp} = xxP^{1/6}n_e^{-1/x}$) and for effective self guiding and self injection the laser power must be maintained well above the critical power for self focusing. Simulations have suggested a power threshold for self injection at low electron densities ($n_e \sim 10^{18}$ cm^{-3}) to be around $P/P_{cr} = 4 - 8$ [13, 17]. This is consistent with experiments where the laser powers are typically limited to < 50 TW within the central laser spot and self injection is reported to be difficult below

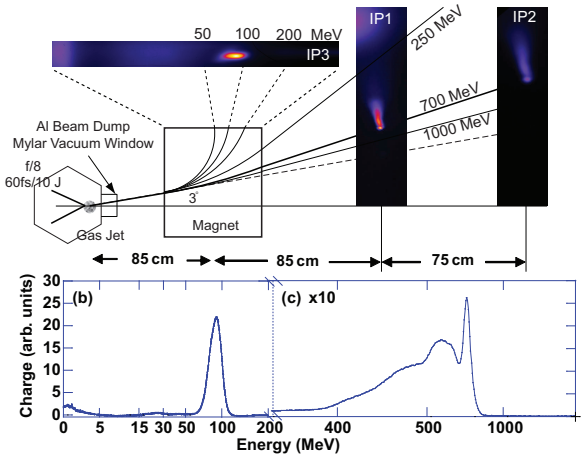

FIG. 1: Two successive image plates (IP1 → IP2) are used to measure the deflection and energy of the electron beams. Low energy electrons (E $\lesssim$ 150 MeV) are deflected out the top of the magnet and are detected by a third image plate (IP3). The spectra show results from an experiment where a peak power of 80 TW produced a 720 ± 50 MeV electron beam with a 3^o deflection; a 90 ± 10 MeV feature is also measured on IP3. The electron spectra measured by (b) IP3 and (c) IP1 are shown where the total charge in the 90 MeV feature was measured to be 34 pC and 6.7 pC for energies above 300 MeV.

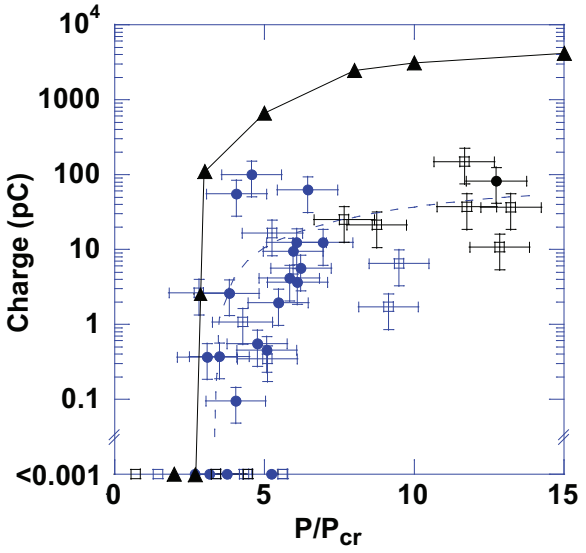

FIG. 2: The total charge accelerated above 250 MeV is shown as a function of P/P_{cr} at two densities (circles) 3×10^{18} cm^{-3} and (squares) 5×10^{18} cm^{-3}. Below $P/P_{cr}<4$ no charge is accelerated beyond 250 MeV. The PIC simulations (triangles) agree well with the measured self-injection threshold. The open (closed) symbols represent results from the 5-mm (8-mm) long gas jets.

$\sim 5\times10^{18}$ cm^{-3}. A study of the trapping threshold at high densities and low electron beam energies was performed [5], but there has been no experimental study to date of this threshold at lower densities where the laser pulse is completely contained within the blow-out region and the electrons are accelerated to high energies.

In this letter, we present the first GeV-class laser wakefield acceleration experiments where a self-injection threshold is demonstrated ($P/P_{cr}>4$) for densities below 5×10^{18} cm^{-3}. For these densities, the laser has been matched to the plasma conditions creating a blown-out, self-guiding accelerating structure over 8 mm. The charge in the quasi-monoenergetic electron beams increases rapidly from 10 pC to a saturation level of $\sim$ 100 pC when P/P_{cr} is increased from 4 to 15. Furthermore, the quasi-monoenergetic electron beam energy is measured to increase from 100 MeV to 700 MeV when the plasma length is increased from 3 mm to 8 mm. These experiments use a novel two-screen electron spectrometer (Fig. 1) to unambiguously measure the charge, energy, and deflection angle of electron beams. These results are well reproduced by full 3D particle-in-cell (PIC) simulations and are also in very good agreement with theoretical predictions [13].

The experiments reported here were performed at the Jupiter Laser Facility, Lawrence Livermore National Laboratory, using the recently upgraded 200 TW ultra-short pulse Ti:Saaphire Callisto Laser System. To maintain the short ($\tau_{FWHM}=60\pm5$ fs) laser pulses the system employs an optical pulse shaper (Sillohuette [18]). Figure 1 shows the experimental setup where the $\lambda=0.81$ micron laser beam was focused, by an $f/8$ off-axis parabola, to the leading edge of a He gas jet. The vacuum spot size was measured at low powers to be $w_0=15$ microns at the $1/e^2$ intensity point which corresponds to a Raleigh length of $Z_r=\pi w_0^2/\lambda=900$ microns. It is assumed that 50% of the energy is outside of the central spot therefore, for a maximum energy of 13 J over 60 fs, a peak power of 100 TW is achieved corresponding to a peak vacuum intensity of 2×10^{19} W-cm^{-2} or a normalized vector potential of $a_o=3.5$.

Three super-sonic gas jets were carefully designed to produce uniform density profiles over 3 mm, 5 mm, and 8 mm [19]. The density profiles where characterized using low laser powers to ionize the He gas and a Lloyd mirror interferometer that employed a 100 fs probe beam. The error in absolute density is estimated to be $\pm1\times10^{18}$ cm^{-3} [14].

The electron beams produced by this laser wakefield accelerator were characterized using the two-screen spectrometer shown in Fig. 1 which provides an accurate measurement of the electron charge, divergence, energy and deflection [20]. The electrons propagating out of the plasma pass through a 40 micron thick aluminum optical beam dump and a 62.5 micron thick mylar vacuum barrier before being deflected by a 0.46 Tesla magnetic field. The magnetic field is produced by two 20 cm x 8 cm permanent magnets separated by 3.5 cm. Electrons with energies less than $\sim$ 200 MeV are deflected onto an image plate placed against the top of the magnet (IP3). Electrons with sufficient energies to propagate through the magnet are detected by two successive image plates (IP1 $\rightarrow$ IP2) providing a unique solution to their energy and deflection angle through the relativistic equations of motion [21]. Furthermore, the image plates have been calibrated to provide a direct measure of the electron charge [22] within a 35 mRad collection angle. For electron energies of interest in this study (above 25 MeV), the system can detect less than 0.001 pC of charge.

Figure 2 shows that charge is self-injected and accelerated to high energies when $P/P_{cr}\gtrsim4$. The data shown in this plot spans a range of peak laser powers (5 TW - 100 TW) and plasma densities less than 5×10^{18} cm^{-3}. Below the critical power for self-injection, less than 0.001 pC of charge are detected at energies above 150 MeV while above this threshold the charge increases rapidly to saturation ($\sim$ 100pC). The charge measured in these experiments can be characterized as having three spectral features which are evident in the spectra shown in Fig. 1: low-energy thermal tail (<50 MeV), self-trapped low-energy beam (25 MeV $-$ 150 MeV), and self-trapped high-energy peak (>150 MeV). The low-energy thermal tail has a large divergence and is therefore not correctly resolved by our spectrometer. This part of the spectrum has been subtracted from all charge measurements.

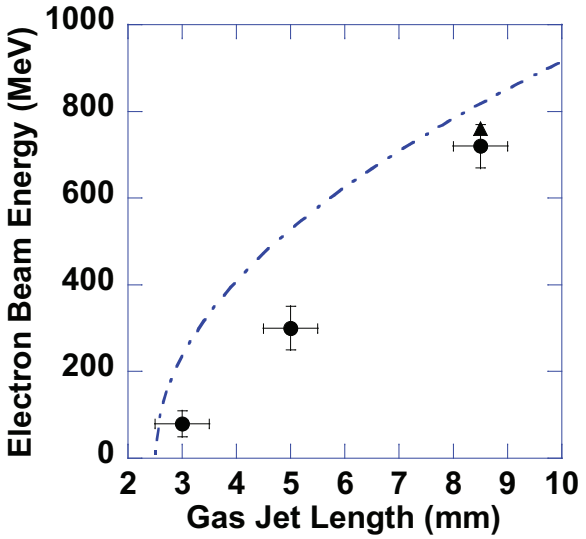

FIG. 3: The measured energy gain as a function of plasma length is plotted for a constant peak laser power (70±15 TW) and plasma density (3×10^{18} cm^{-3}). These measurements are compared with full 3D PIC simulations (triangles) [need to include more points from simulations].

Figure 3 shows that as the plasma length is increased from 3 mm to 8 mm, the electron beam energy increases by a factor of 7. This increase in energy over 5 mm ($6\times Z_r$) indicates that the laser is self-guided and an accelerating structure with a nearly constant electric field is produced over this entire length. The 700 MeV feature has a divergence of $\Delta\theta_{FWHM} = 2.85\pm0.15$ mRad measured by the first image plate (IP1). Using the source size measured in from the PIC simulations ($\sigma_r \simeq 1$ μm), a corresponding normalized emittance of $\epsilon = \sigma_r\gamma\Delta\theta =$ 5 mm-mRad is estimated. Monte Carlo simulations using the code ITS [23] indicate that the electron divergence resulting from the scattering through the 40 micron thick Al, 62.5 micron thick Mylar, and 100 cm of air is $\Delta\theta_{FWHM} < 0.25$ mRad for an electron energy of 700 MeV.

Figure 4 shows the results from PIC simulations where the laser beam completely blows-out the electrons producing a stable accelerating structure. In these simulations it is evident that the laser system is well matched to the plasma conditions as the laser pulse is completely contained within the ion-sphere. Furthermore, the initial conditions from the experiment are well matched for self-guiding. The laser beam is focused at the edge of the density plateau and initially self-focuses to 8 microns before expanding over one Rayleigh length to the matched laser spot size ($w_m[\mu m] \cong 8.5\times 10^6\,(\mathrm{P\ [TW]})^{1/6}\left(\mathrm{n}_e[\mathrm{cm}^{-3}]\right)^{-1/3} = 13\mu$m). After this initial evolution, self-injection occurs and electrons are accelerated to high energies; 6 mm into the simulation, the highest energy electrons begin to dephase and a 760 MeV quasi-monoenergetic electron bunch is produced (Fig. 3), which is in good agreement with the simple theoretical estimates given by E [GeV] $\simeq 1.7\,(\mathrm{P/100\ TW})^{1/3}\left(10^{18}\ \mathrm{cm}^{-3}/\mathrm{n}\right)^{2/3} = 0.8$ GeV [13]. The divergence of the high energy beam is measured to be 2 mRad which compares well with the experimental observations.

The PIC simulations were performed in 3 dimensions using the code OSIRIS [24] and initialized with the experimental parameters ($\tau_{FWHM} = 60$ fs, $w_0 = 15$ μm, P=100 TW). The initial He gas profile consistent with the measured 8 mm density plateau was used [Fig. **??**(a)]; the density increased linearly from vacuum to the plateau density ($\mathrm{n}_e = 3\times10^{18}$ cm^{-3}) over 500 microns. The simulations used a 100 μm$\times$150 μm$\times$150 μm computational window corresponding to $4000\times256\times256$ gridpoints with a resolution along the laser propagation direction of 25.4 nm and 595 nm in the transverse plane and 4 particles per cell.

In order to find the self-injection threshold numerous PIC simulations were necessary therefore, a newly developed capability was used that allows for the computation to be performed in a boosted frame [25, 26]. For our parameters, using a moving frame with a relativistic factor $\gamma = 5$ provided a factor of 20 reduction in simulation time, thus allowing us to obtain 8 simulation points shown in Fig. 2.

Figure 2 compares the electron charge accelerated to high energy from the simulations with the experiments. Although the simulations reproduce the threshold and the charge around the threshold, they quickly over estimate the charge accelerated to high energies as the power goes above threshold. We speculate that this could be a result of the inevitable imperfections present in high power laser spots, density fluctuations in the gas profiles, or not sufficient resolution in the simulations. This warrants further work as high power laser systems are coming on line and are likely to operate significantly above the self-trapping threshold.

An estimate of the trapping threshold can be determined by equating the phase velocity of the wake ($v_\phi \simeq \mathrm{c}[1-3\mathrm{n}/2\mathrm{n}_c]$) to the velocity of the electrons propagating along the sheath and accelerated towards the laser axis. The energy gained by the electrons as they approach the back of the bubble is given by the electric field just inside the bubble $\mathrm{E} = \mathrm{enR}/2\epsilon_0$ where $\mathrm{R} = 2\sqrt{2}\mathrm{c}/\omega_p(\mathrm{P}/\mathrm{P}_c)^{1/6}$ [13]. As the electrons converge at the back, they produce a charge density spike that can be approximated by $\delta\mathrm{n} \simeq 2\mathrm{n}\gamma^2$ [11]. This charge density results in an increased potential, giving an additional boost that can self-inject electrons. The final energy of the electrons accelerated by this process can be expressed as

$$\gamma = 4\left(\frac{\mathrm{P}}{\mathrm{P}_{cr}}\right)^{1/3}\left[1+64\left(\frac{\Delta}{\mathrm{R}}\right)^2\left(\frac{\mathrm{P}}{\mathrm{P}_{cr}}\right)^{2/3}\right] \qquad (1)$$

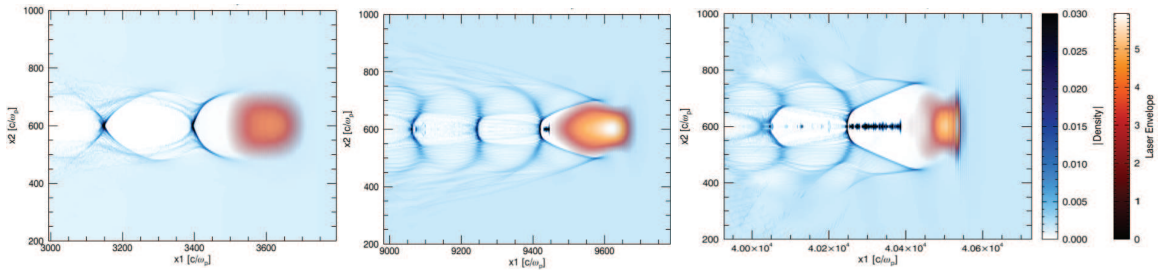

FIG. 4: (a) A snap shots of the density profiles (blue color table) from the simulation are shown initially at z=0.5 mm, where laser pulse has completely blown out the electrons forming a nearly spherical wakefield. (b) As the system evolves, a stable accelerating structure is formed and self-injection occurs (z=3 mm). (c) By the end of the plasma (z=8.5 mm), the highest energy electrons have begun to dephase producing a quasi-monoenergetic 760 MeV electron beam. The laser pulse is super imposed on the density map (red color table).

where $\gamma = 1/[1-(v/c)^2]^{1/2}$ and $\frac{\Delta}{R} \sim 0.1$ is the typical width of the sheath normalized to the radius of the bubble [10]. Equation refeqn1 shows that increasing the laser power increases the self-trapping threshold through increasing both the energy gained by the electrons due to the increased in wakefield (first term) and the increased charge density at the rear of the bubble (second term) while reducing the density not only reduces both of these terms but has the added effect of increasing the phase velocity of the wake making trapping more difficult. We note that for densities above $\sim 5\times10^{18}$ cm^{-3} and a reasonable laser power (100 TW), the first term is sufficient to satisfy the condition for self-trapping. However, once the density is reduced below this point the electrons require the extra boost from the density spike.

For the densities explored in this study, around 0.2% of the critical density, the phase velocity of the wake is $v_\phi/c = 0.997$ ($\gamma_\phi = 13$). Equation 1 then gives a self-trapping threshold ($\gamma = \gamma_\phi$) at $P/P_c = 3$ which is in qualitative agreement with Fig. 2.

In summary, we have used a 200 TW short-pulse laser to demonstrate a threshold for electron self-injection ($P/P_{cr} \simeq 4$) at low densities (3×10^{18} cm^{-3}) in a laser wakefield accelerator experiment. The electron energy gain was measured to increase linearly with plasma length, from 100 MeV at 3 mm to 700 MeV at 8 mm. The combination of the high electron beam energy with a low emittance ($\epsilon = 5$ mm-mRad) suggests that our experiments produced a stable guiding structure which is supported by full 3 dimensional PIC simulations.

We would like to thank B. Stuart, D. Price, S. Maricle, and J. Bonlie for their contributions to upgrading the Callisto Laser System for this experiment. This work performed under the auspices of the U.S. Department of Energy by Lawrence Livermore National Laboratory under Contract DE-AC52-07NA27344 and a Department of Energy Grant No. DEFG03-92ER40727 (UCLA) and was partially funded by the Laboratory Directed Research and Development Program under project tracking code 06-ERD-056.

* Electronic address: froula1@llnl.gov

[1] T. Tajima and J. M. Dawson, Phys. Rev. Lett. **43**, 267 (1979).
[2] C. E. Clayton *et.al.*, Phys. Rev. Lett. **70**, 37 (1993).
[3] C. A. Coverdale*et.al.*, Phys. Rev. Lett. **74** (1994).
[4] A. Modena *et.al.*, Nature **377**, 606 (1995).
[5] D. Umstadter *et.al.*, Science **273** (1996).
[6] V. Malka *et.al.*, Science **298**, 1596 (2002).
[7] C. Geddes *et.al.*, Nature **431**, 538 (2004).
[8] J. Faure *et.al.*, Nature **431**, 541 (2004).
[9] S. Mangles *et.al.*, Nature **431**, 535 (2004).
[10] W. Lu *et.al.*, Phys. Rev. Lett. **96** (2006).
[11] W. Lu *et.al.*, Phys. Plasmas **13** (2006).
[12] G. Z. SUN *et.al.*, Phys. Fluids **30**, 526 (1987).
[13] W. Lu *et.al.*, PRSTB **10**, (2007).
[14] J. E. Ralph *et.al.*, Phys. Rev. Lett. **In Print** (2009).
[15] A. Thomas *et.al.*, Phys. Rev. Lett. **98**, (2007).
[16] N. Hafz *et.al.*, Nature Photonics **2**, 571 (2008).
[17] F. Tsung *et.al.*, Phys. Plasmas **13**, (2006).
[18] V. V. Lozovoy *et.al.*, Opt. Lett. **29**, 775 (2004).
[19] V. Malka *et.al.*, Rev. Sci. Instr. **71** (2000).
[20] B. B. Pollock *et.al.*, in *In Print, Proceedings of the Particle Acceleration Conference* (Vancouver, Candida, 2009).
[21] I. Blumenfeld *et.al.*, Nature **445**, 741 (2007).
[22] N. Nakanii *et.al.*, Rev. Sci. Instr. **79**, 066102 (2008).
[23] B. C. Franke, Tech. Rep. SAND2004-5172, Sandia National Laboratories (2005).
[24] R. A. Fonseca *et.al.*, in *ICCS 2002* (P.M.A., 2002), pp. 342–351.
[25] J.-L. Vay, Phys. Rev. Lett. **98** (2007).
[26] S. F. Martins *et.al.*, To be submitted (2009).